Check for updates

Adsorption Science & Technology

Research Article

Adsorption Science & Technology
2018, Vol. 36(3–4) 936–952
© The Author(s) 2017
DOI: 10.1177/0263617417733586
journals.sagepub.com/home/adt
SAGE

Adsorption isotherms and kinetics of vanadium by shale and coal waste

George William Kajjumba, Serdar Aydın and Sinan Güneysu
Department of Environmental Engineering, Istanbul University, Istanbul, Turkey

Abstract

The use of adsorption using nanomaterials has become a very competitive method for removal of hazardous materials from wastewater. With increasing consumption of fossil fuels and development of energy storage systems, the levels of vanadium pollution are expected to increase. Utilizing natural shale and coal waste as adsorbents, batch adsorption, isotherms, and kinetics of vanadium was studied. The adsorption characteristics of shale and coal waste were studied using Fourier Transform Infrared spectroscope and Scanning Electron Microscopy. The effect of pH, the amount of adsorbent, vanadium concentration, temperature, and contact time between adsorbate and adsorbents were also studied to obtain optimum conditions for maximum adsorption of vanadium. The Fourier Transform Infrared results show little distortion in the vibration of bands, and hence the surface properties remain unchanged for both sorbents after adsorption. The adsorption kinetics are best described by pseudo-second order, while Langmuir model fits the adsorption isotherm for both adsorbents. Maximum sorption capacity is 67.57 mg/g for shale while that of coal is 59.88 mg/g at 298 K and pH 3. For both adsorbents, the adsorption process is spontaneous, endothermic, and chemisorption in nature. Both adsorbents can effectively be recycled twice.

Keywords

Vanadium, Fourier Transform Infrared, clay, coal, Gallic method

Submission date: 9 May 2017; Acceptance date: 29 August 2017

Introduction

Vanadium is a rare earth soft metal (0.01% of the earth's crust), silver-grey in colour (Clarke and Washington, 1924). It exists in different forms of oxides and complexes

Corresponding author:
Serdar Aydın, Department of Environmental Engineering, Faculty of Engineering, Istanbul University, Avcilar Campus, Avcilar, Istanbul, Turkey.
Email: saydin@istanbul.edu.trr

Creative Commons CC-BY: This article is distributed under the terms of the Creative Commons Attribution 4.0 License (http://www.creativecommons.org/licenses/by/4.0/) which permits any use, reproduction and distribution of the work without further permission provided the original work is attributed as specified on the SAGE and Open Access pages (https://us.sagepub.com/en-us/nam/open-access-at-sage).

(−1, 0, +2, +3, +4, +5) with vanadium pentoxide being the most stable state (Sirviö et al., 2016). Apart from its own ores, vanadium oxides are extracted from iron and uranium ores and the salt roast process (Zakrzewska-Koltuniewicz et al., 2014). Currently, the main source of environmental contamination by vanadium is combustion of fuels. It is estimated that 69,000 tons are released into the atmosphere annually (Costigan et al., 2001). The typical concentration of vanadium in crude fuels ranges from 0.2 μg/g to 260 μg/g and 14 mg/kg to 56 mg/kg in coal (Costigan et al., 2001; Fernández-Álvarez et al., 2007). After combustion, varying quantities of vanadium remain in solid residues, soot, fly ash, and boiler scale as vanadium pentoxide. Vanadium is used in power grid systems as an energy storage material (Parasuraman et al., 2013). With increasing consumption of such fuels and development of energy storage systems, the levels of vanadium pollution are also expected to increase. Pollution of water bodies and the soil could also easily occur if vanadium sediments were subjected to acidic conditions (pH $\leq$ 2) (Cappuyns and Swennen, 2014).

After the price fall of major minerals in 2015, the price of vanadium has steadily increased to USD 21/kg (infomine.com, 2016). This is due to increased production of steel, high-speed aircraft, jet engines, and production of superconducting magnets of which vanadium is a requirement (Moskalyk and Alfantazi, 2003). In addition, due to the development of renewable energy systems, vanadium demand is expected to escalate since it has been identified as a superior energy storage material (Parasuraman et al., 2013). Vanadium retains its charge over a longer period of time compared to lithium (Tarascon and Armand, 2001). In animal cells, vanadium is essential for stimulation of vascular permeability factor which is responsible for the creation of new or rebuilding lesion blood vessels (Korbecki et al., 2012). However, vanadium has diverse effects in mammals and birds. For example, increased concentration of vanadium (5–10 mg/kg) reduces egg albumen quality (Wang et al., 2017). Vanadium compounds (sodium metavanadate) at elevated levels cause epididymis weight loss, sperm count loss in males, eye irritation and increases neoplastic cell growth (Llobet et al., 1993; Roberts et al., 2016).

Different methods have been researched and developed for the recovery and reduction of vanadium pollution, these include: ion exchange resins (Gomes et al., 2016; Yeom et al., 2009); leaching (Cappuyns and Swennen, 2014; Chen et al., 2010); and gravity separation (Zhao et al., 2013). However, leaching process requires elevated concentration of the acid and temperatures (Cappuyns and Swennen, 2014), while ion exchange is not a desirable method for removing low metal concentrations (Uddin, 2017). By the use of adsorption using nanomaterials, adsorption method has become a competitive and cost-effective method for removal of organics, metals, and dyes from solutions. Adsorption method has a high efficiency for removal of organic and inorganic contaminants (Smith and Rodrigues, 2015). The choice of any adsorbent depends mainly on adsorption capacity, cost, availability, and reusability.

Removal of vanadium from solution presents a challenge for many countries owing to high cost of existing technologies and adsorbents. Recently, vast modified adsorbents (activated carbon, sludge, chitosan) have been studied to effectively recover vanadium (Doğan and Aydın, 2014; Mthombeni et al., 2016; Sharififard and Soleimani, 2015; Sirviö et al., 2016). However, the shortcomings of most of these adsorbents are high operational and maintenance costs, generation of toxic and complicated procedure involved in making them. Although traditional adsorbents like shale and coal waste have been studied for removal of different metals, vanadium adsorption by these adsorbents has received less

attention (Uddin, 2017). The adsorption characteristics of vanadium on such adsorbents are not well known.

Shale is extensively distributed over the earth's surface – mainly composed of silica, alumina, hydroxyl, and weathered rocks (Chamley, 1989; Uddin, 2017). Clays (bentonite, zeolite, pyrrole, and vermiculite) have received great attention in the past decades due to their ability to immobilize trace and heavy metals in soil (Chen et al., 2015; Mthombeni et al., 2016; Wang et al., 2017). Clays are able to achieve this due to their electrochemical properties, large surface area, and large pore volume (Leroy and Revil, 2004; Uddin, 2017). Due to the limited isomorphic exchange in the octahedral and tetrahedral sheets, shale is always negatively charged (Leroy and Revil, 2004). This makes shale a desirable material for cation adsorption. Combining these factors and the fact that shale is far less toxic, is abundantly available, and a less expensive material, shale is ideal for adsorption of vanadium.

Although coal processing and production produce a vast amount of wastes and pollutants, its overall consumption is expected to increase (Höök et al., 2010). As of 2014, the global consumption of coal ranged between 5 and 6 Gt (United Nations, 2016). Of this, 10–15% is estimated to be coal waste (Haibin and Zhenling, 2010). According to Ribeiro et al. (2010), coal wastes from the unburnt piles constitute mainly illite and quartz, while those from the burnt zone contain illite, quartz, mullite, jarosite, and a significant amount of amorphous material. Coal waste has been recycled in different forms, these include: coal ash can act as a bidder material in construction (Kacimi et al., 2010; Mohammadinia et al., 2017), ceramic and glass industry (Blissett and Rowson, 2012; Zhang et al., 2007), soil amelioration due to its buffering characteristics (Bolan et al., 2014; Ukwattage et al., 2013). Upon modification, coal waste has been successfully used as an adsorbent (Blissett and Rowson, 2012; Cardoso et al., 2015; Mohan and Gandhimathi, 2009). While waste coal has been recycled in different ways, tons of unburnt coal waste are disposed off in landfills (Haibin and Zhenling, 2010).

As the world is looking for better ways of recycling coal waste and cheap means of recovering vanadium, shale and unburnt coal waste as adsorbents need to be investigated. Therefore, the aim of this study was to develop accurate, reliable, and convenient quantitative data for the use of shale and coal as adsorbent materials for vanadium. The study investigates the adsorption properties of shale and unburnt coal waste in the abstraction of vanadium from the water. Adsorption kinetics and equilibrium conditions are also studied to understand the behaviour of vanadium adsorption.

Materials and methods

Material characterization

Shale and unburnt coal waste were collected from Trakya mining region, Turkey (GPS coordinates: 41.141968N, 28.353888E for shale and 41.143356N, 28.352600E for coal). Materials were air-dried, crushed, and then sieved to give 0.5–1.0 mm particles using ASTM standard sieves. The particles were washed with distilled water, dried for 24 hours at 105 °C in the oven. Then the Brunauer–Emmett–Teller (BET) specific surface area, micropore volume, and size were measured using Quantachrome Autosorb IQ Automated Gas Sorption Analyzer. The total pore volume was measured for pores smaller than 1199.7 Å at $P/P_0 = 0.99195$. The alpha Fourier Transform Infrared (FTIR) spectrometer patterns were used to study the functional groups of the adsorbents. Scanning Electron Microscopy

(SEM) JEOL/JSM-6610 model was used to study the morphology of the adsorbents. The results from the FTIR were analysed using *Origin* 94E software. The adsorption of vanadium was studied using FTIR and SEM.

Calibration curve

The standard graph for estimation of vanadium concentration (Figure 1(a)) was developed using the Gallic acid method (Fishman and Skougstad, 1964). Ammonium monovanadate (NH_4NO_3) was used as a source of vanadium and was supplied by Merck Chemicals. Beer's law of absorbance is applied, that is, the oxidation of Gallic acid is proportional to the concentration of vanadium in the solution. The wavelength was set at 415 nm. The absorbance strength was measured using Spectroquant Pharo 300 spectrophotometer.

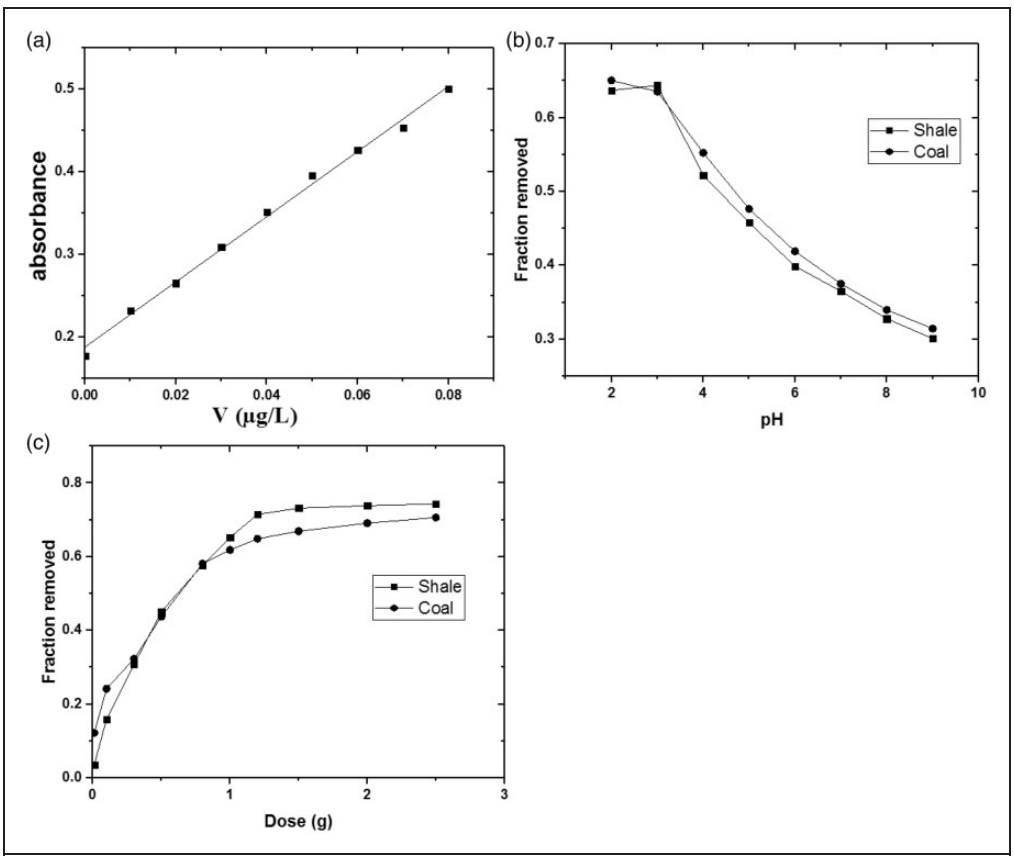


Figure 1. Calibration curve (a), effect of pH on adsorption (b), and effect of dosage on adsorption (c) of vanadium.

Batch adsorption, isotherms, and kinetics

Batch adsorption was studied by agitating 1.5 g of coal waste and 1.2 g of shale with 50 mL of vanadium solution at varying concentration (40–100 mg/L of vanadium). The effect of pH is examined by varying the pH from 2 to 9 of 50 mL (100 mg/L of vanadium) with 1.0 g of each adsorbent. Furthermore, the effect of temperature was studied by adjusting the temperature between 15 °C and 40 °C of 50 mL (100 mg/L of vanadium). The flasks and their contents were shaken for 24 hours at 120 r/min. To determine the fraction of vanadium removed, samples were picked, filtered and residual vanadium was determined using the Gallic acid approach. Applying equation (1), the fraction of vanadium removed from the solution was determined

$$\text{Fraction removed} = \frac{(C_0 - C_e)}{C_0} \tag{1}$$

while adsorption equilibrium capacity is determined using equation (2)

$$q_e = \frac{(C_0 - C_e)}{m} \times V \tag{2}$$

where C_0 is the initial concentration (mg/L), C_e is the equilibrium concentration (mg/L), q_e is the equilibrium amount of vanadium adsorbed (mg/g), while m is the sorbent mass (g). Langmuir (monolayer adsorption), Freundlich (heterogeneous adsorption), and Dubinin–Radushkevich (homogenous and heterogeneous surface) models were studied to investigate the adsorption isotherms of vanadium (Doğan and Aydın, 2014). The adsorption kinetics of vanadium on the adsorbents were analysed using pseudo-first-order and second-order kinetics. Intra-particle model was used to further investigate the time-dependent adsorption capacity of coal waste and shale.

Regeneration

For economic purposes, regeneration of the adsorbents was investigated. Shale (1.2 g) and coal waste (1.5 g) were made to contact with 50 mL of 100 mg/L of vanadium. Used adsorbents were agitated with 20 mL of 1 M NaOH for 24 hours at 25 °C. After the adsorbents were mixed with 20 mL of 1 M HNO_3 for 2 hours (Mthombeni et al., 2016), the adsorbents were dried, weighed, and reused. The process was repeated five times for each adsorbent. The adsorption capabilities were measured using equation (2).

Results and discussion

Characteristics of the adsorbent

The FTIR spectra of shale and coal waste before adsorption are shown in Figures 2(b) and 3(b), respectively. For both adsorbents, the bold peaks at 3380 are due to elongation of O–H, O–H–O, and amine functional groups. In coal waste, the vibration at 2926, 1738, 1630, 983, and 776 (Figure 3(b)) is due to the stretching of C–H, C = O, C = C, Si–O–Si and Si–O–Na bands, respectively (Balachandran, 2014; Goswami et al., 2017; Ren et al., 2015). The shale's FTIR (Figure 2(b)) shows peaks at 1712, 1621, 1433, 996, and 830. These peaks correspond to C = O, C = C, S = O, Si–O, and Al–OH–Fe, respectively (Herbert et al., 2016).

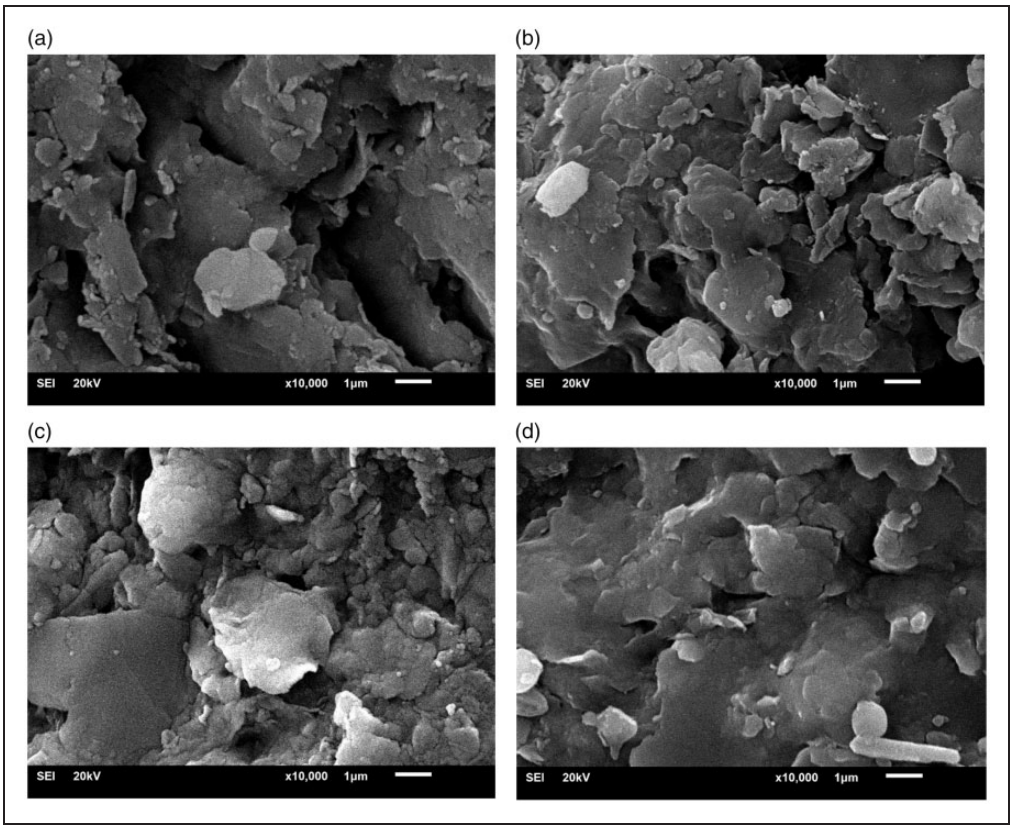


Figure 2. FTIR spectrum of shale before (b) and after (a) adsorption of vanadium.

After sorption, there is a shift in the vibration of some bands. For coal, 1738, 1630, 1432, 1366, and 983 wave spectrum shifted to 1740, 1623, 1446, 1373, and 992, respectively (Figure 3(a)). In addition, visible peaks are formed at 1717 and 828 wavelength. While for shale, peaks 3365, 1433, 1202, and 643 shifted to 3398, 1416, 1275, 676, respectively. Moreover, incipient peaks are detected at 1566 cm^{-1} and 753 cm^{-1} for shale (Figure 2(a)).

These new peaks correspond to stretching of V = O at a high wavelength, while those between 750 and 1000 spectra are attributed to vibration of V–O bands (Mthombeni et al., 2016). The shifting and formation of incipient peaks confirm the adsorption of vanadium on both adsorbents. Comparing the FTIR results before and after adsorption for both adsorbents, there was a little distortion of the adsorbents, thus the surface properties remain unchanged. This can also be confirmed from SEM images (Figure 4(a) to (d)). There was no major change in the morphology of the adsorbents after adsorption. Comparing the SEM images of shale (Figure 4(c)) and coal waste (Figure 4(a)), shale had a better dispersibility, which was conducive for adsorption. From BET results (Table 1), shale has a large surface area and bigger micropore volume compared to coal. These factors facilitate easier adsorption by shale than coal waste. Unlike the previous studies, no surface activation and pretreatment were applied to the adsorbent samples (Doğan and Aydın, 2014; Mthombeni et al., 2016; Sharififard and Soleimani, 2015).

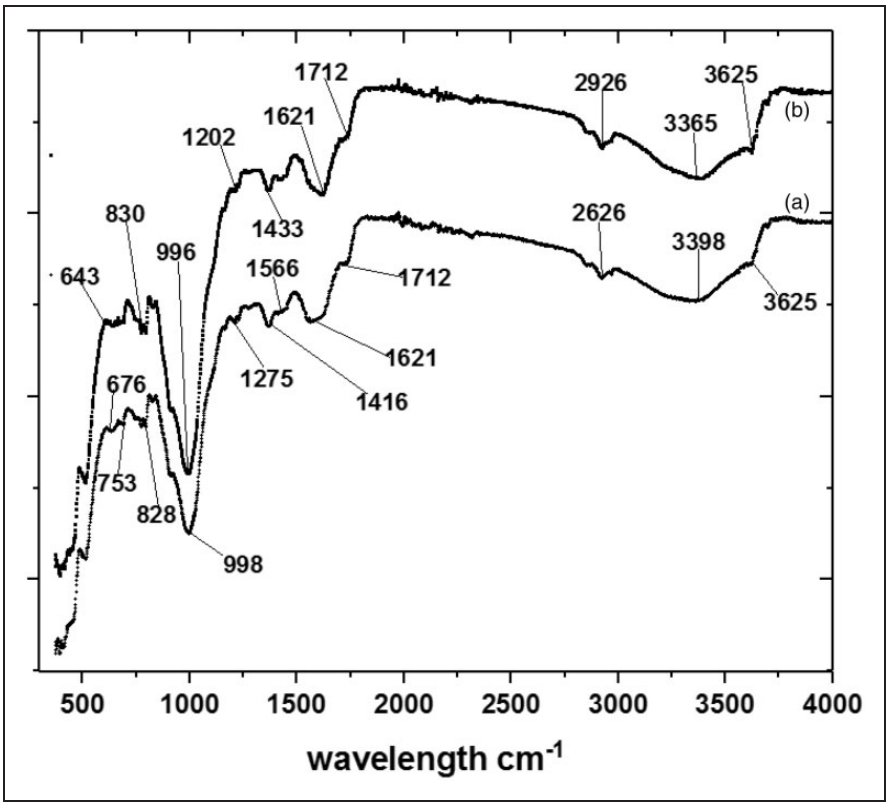


Figure 3. FTIR spectrum of coal before (b) and after (a) adsorption of vanadium.

Effect of pH and adsorbent quantity

The influence of pH on the abstraction of vanadium was investigated by agitating 1.0 g of each adsorbent with 50 mL of 100 mg/L of vanadium. The pH was adjusted to 2, 3, 4, 5, 6, 7, 8, 7, and 9. According to Figure 1(b), an increase of pH above 3 showed a decrease in the abstraction of vanadium by both adsorbents. At $pH \leq 3$, the major form of vanadium is pentavalent cation VO^{2+}, while at $3 < pH < 5$, pentavalent anions, VO_3^- is the major species of vanadium in the solution (Yu et al., 2017). Therefore, the decrease in adsorption capacity ($3 < pH < 5$) is attributed to the electrostatic repulsion between VO_3^- and the sorbents. Further decrease in adsorption capacity of the adsorbents at $pH > 5$ is attributed to the formation of vanadium polymers that have less removal efficiency (Mthombeni et al., 2016). Figure 1(c) indicates increasing removal of vanadium, as the concentration of the adsorbents is increased from 0.010 g to 2.5 g. This is attributed to the increased number of active sites available. However, increasing the adsorbent dose beyond 1.5 g and 1.2 g for coal waste and shale, respectively, shows little improvement in the adsorption. This can be attributed to the aggregation of adsorbent at high dosage, thus reducing the available adsorption sites (Yu et al., 2017). Hence, pH 3.0, 1.5 g (coal waste), and 1.2 g (shale) were used in the subsequent experiments.

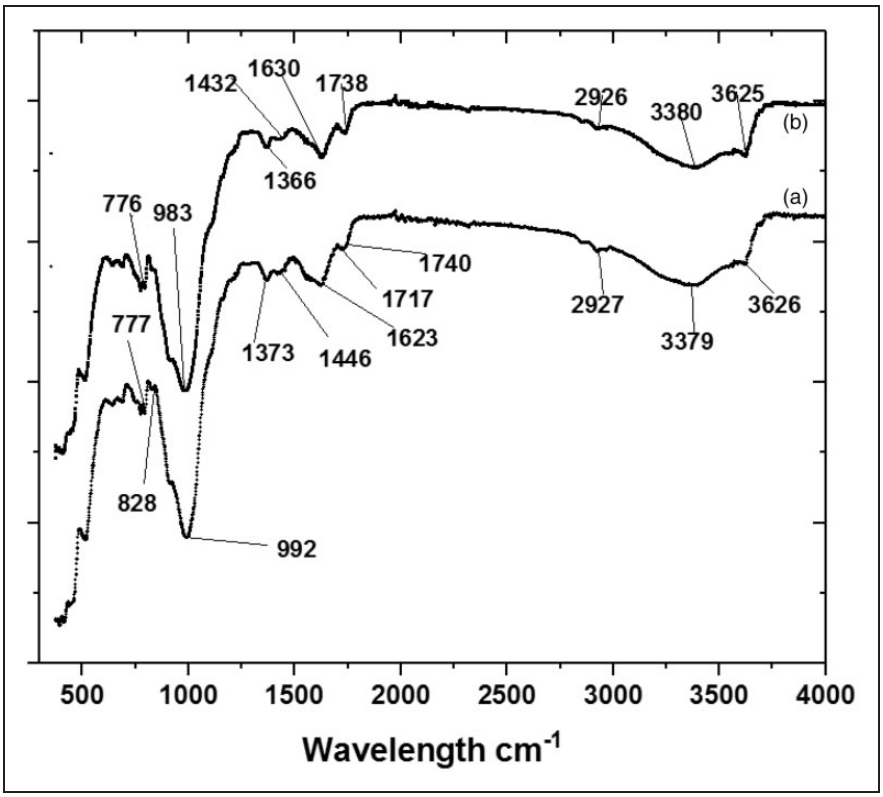


Figure 4. SEM images of coal before (a), after (b) adsorption and shale before (c), after (d) adsorption.

Table 1. BET surface characteristics.

	Surface area (m^2/g)	Micro-pore volume (cc/g)	Pore radius (Å)
Shale	3.322	0.0211	126.80
Unburnt coal waste	1.966	0.0166	169.34

Adsorption kinetics

The pseudo-first-order equation (3) and pseudo-second-order equation (4) were applied to examine the kinetics of vanadium on shale and coal waste (Sirviö et al., 2016)

$$q_t = q_e(1 - e^{-k_1 t}) \tag{3}$$

$$q_t = \frac{q_e^2 k_2 t}{1 + q_e k_2 t} \tag{4}$$

$$q_t = K_p \sqrt{t} + C \tag{5}$$

where q_t is the amount of vanadium ions adsorbed at time t (mg/g), q_e is the adsorption capacity at equilibrium (mg/g), k_1 and k_2 are pseudo-first-order and second-order rate constants (L/min), K_p is an intra-particle diffusion equilibrium, C is the initial adsorption of internal diffusion related to boundary thickness, and t is the contact time (min).

Figure 5(a) and (b) shows the effect of initial concentration of vanadium and the contact time. As the concentration of vanadium increased, the adsorption capacity also increased. The sorption of vanadium was very rapid during the first 120 minutes. This was attributed to readily available sites on the adsorbents and after the equilibrium was attained. Table 2 summaries the kinetic parameters of each model. The analysis of correlation coefficients (R^2), adsorption of vanadium by both adsorbents is best described by pseudo-second order. Consequently, the adsorption of vanadium follows chemisorption process (Doğan and Aydın, 2014; Sirviö et al., 2016). The pseudo-second-order plots are shown in Figure 5(c) and (d) for shale and coal, respectively. The time-dependent adsorption capacity was analysed utilising the intra-particle diffusion model, equation (5). The values of C indicate that shale has a higher boundary layer resistance between the adsorbent and adsorbate compared to coal waste. From Figure 5(e) and (f), the adsorption of vanadium on both adsorbents is not linear during the entire process. Analysis of R^2 shows that the intra-particle diffusion does not fully explain the adsorption of vanadium. Therefore, more than one mechanism was involved in the adsorption of vanadium by both adsorbents.

Adsorption isotherm and nature

The vanadium adsorption isotherms on shale and coal waste were examined using Langmuir, Freundlich, and Dubinin–Radushkevich models (Doğan and Aydın, 2014; Wei et al., 2017). Equations (6) to (9) were applied to investigate the Langmuir, Freundlich, and Dubinin–Radushkevich models, respectively, at 15 °C, 25 °C, and 40 °C

$$q_e = \frac{Q_m b C_e}{1 + b C_e} \tag{6}$$

$$q_e = K_F C_e^{1/n} \tag{7}$$

$$\ln q_e = \ln q_{RD} - \beta \varepsilon^2 \tag{8}$$

$$\varepsilon = RT \ln\left(1 + \frac{1}{C_e}\right) \tag{9}$$

where q_e is the equilibrium amount of vanadium adsorbed (mg/g); Q_m is the Langmuir theoretical monolayer adsorption capacity (mg/g); b is the affinity coefficient (L/mg); C_e is the equilibrium concentration (mg/L); K_F and $1n$ are Freundlich's constants related to capacity (L/g) and affinity of adsorption, respectively, q_{RD} is Dubinin–Radushkevich's monolayer capacity (mg/g), β is the activity constant related to sorption energy (mol^2/kJ^2), ε is the Polanyi potential (kJ/mol), R is the gas constant (8.314 J/mol/K), and T is the absolute temperature (K).

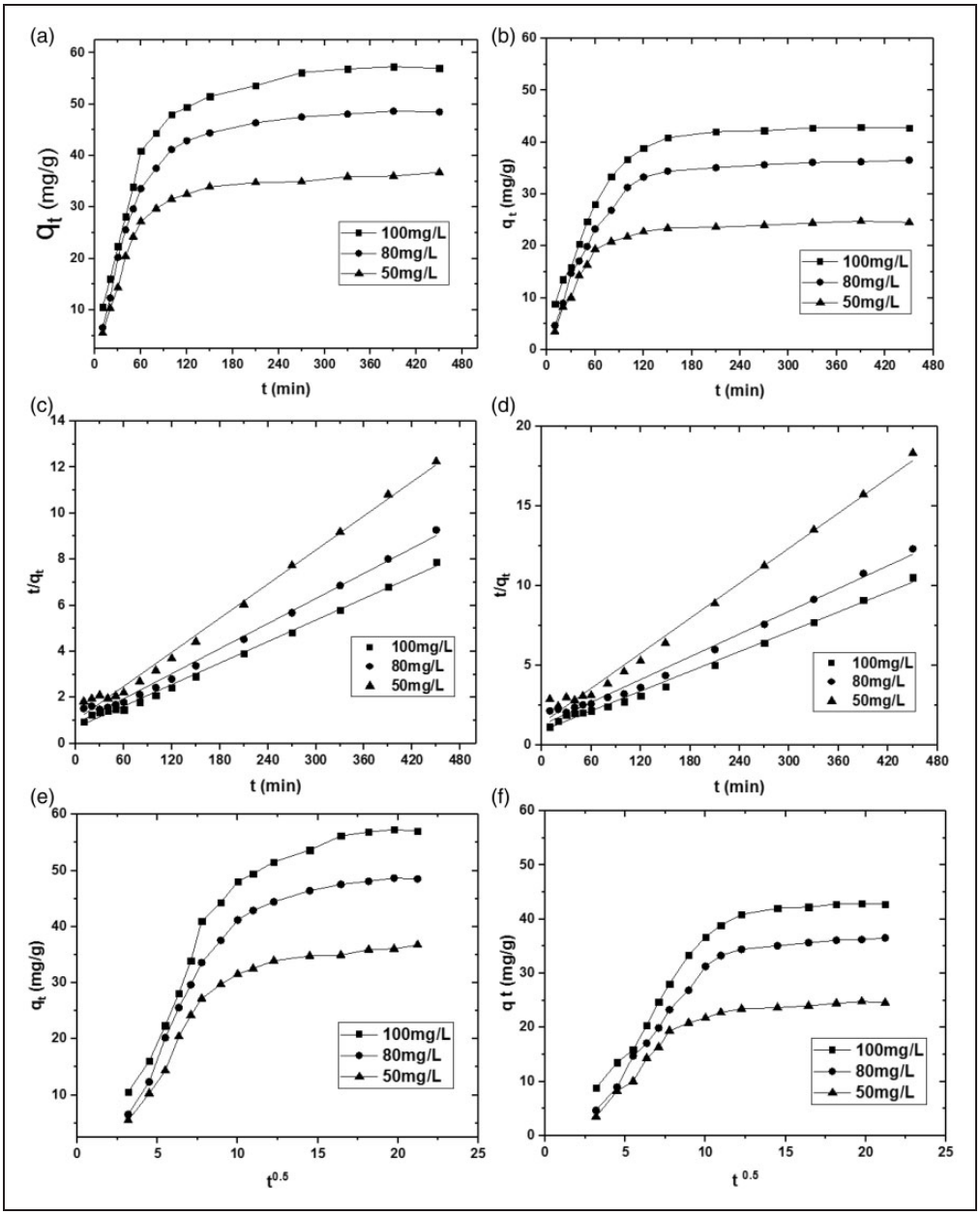


Figure 5. Adsorption kinetics of shale (a), coal (b); pseudo-second order of shale (c), coal (d); intra-particle diffusion model of shale (e), coal (f) for adsorption of vanadium.

The adsorption isotherms were studied at 15 °C, 25 °C, and 40 °C. Figure 6(a) and (b) shows an increase adsorption capacity as temperature increased for shale and coal, respectively. Figure 6(c) and (d) shows experimental results and each model's results plotted together, while Table 3 summaries the models' parameters. Although the

Table 2. Adsorption parameters.

Coal	Pseudo-first order			Pseudo-second order			Intra-particle		
C_0(mg/L)	k_1	q_e(mg/g)	R^2	k_2	q_e(mg/g)	R^2	K_p	C	R^2
50	.0438	16.36	.733	.0010	27.25	.992	1.00	7.74	.707
80	.0055	22.22	.803	.0005	42.02	.990	1.67	7.78	.784
100	.0069	23.90	.830	.0005	48.08	.995	1.87	10.9	.789
Shale									
50	.0101	22.01	.933	.0006	40.49	.993	1.51	10.45	.735
80	.0062	28.05	.865	.0004	54.95	.993	2.12	12.05	.775
100	.0088	34.79	.933	.0004	64.10	.996	2.45	14.52	.795

adsorption capacity increased for all models as temperature increased from 15 °C to 40 °C, assessing R^2 values shows that the Langmuir model describes the adsorption isotherm of vanadium on both adsorbents best. The adsorption capacity of coal waste increased from 55.67 mg/L to 61.35 mg/L as the temperature increased from 15 °C to 40 °C for the Langmuir model (Figure 6(f)). While for shale it increased from 65.79 mg/L to 75.19 mg/L (Figure 6(e)). Therefore, the adsorption processes were endothermic in nature. The high adsorption capacity of shale is due to its large surface area and pore volume when compared to coal.

To further understand the adsorption of vanadium by the adsorbents, dimensionless parameter, R_L (equation (10)) at $C_0 = 100$ mg/L of vanadium, mean adsorption energy (equation (11)), enthalpy, and entropy (equation (12)) were determined

$$R_L = \frac{1}{1 + bC_0} \tag{10}$$

$$E = \frac{1}{\sqrt{2\beta}} \tag{11}$$

$$\mathrm{In}(b) = -\frac{\Delta H^0}{RT} + \frac{\Delta S^0}{R} \tag{12}$$

where E is the mean adsorption energy (kJ/mol), ΔH^0 is the enthalpy change (kJ/mol), and ΔS^0 is the entropy change (J/mol/K). The values $0 < R_L < 1$ indicate favourable adsorption, whereas $R_L > 1$ indicates unfavourable adsorption (Goswami et al., 2017). From Table 3, all R_L values are between 0 and 1 at different temperatures for both adsorbents, implying that adsorption was a favoured mechanism. In addition, the values of $\Delta H^0 > 0$ shows that adsorption was endothermic in nature for both materials. The measure of the degree of randomness (entropy) of the particles on the surface of the adsorbents shows that coal has a higher entropy than shale. Both entropy and enthalpy values are positive; denoting that adsorption of vanadium by both sorbents is favoured at high temperatures (Chen et al., 2015). For $E \leq 8$ kJ/mol, physical adsorption is said to be favoured, while $8 < E \leq 16$ kJ/mol, chemisorption is favoured (Doğan and Aydın, 2014). From Table 3, both adsorbents on average $E > 8$ kJ/mol thus chemisorption was favoured.

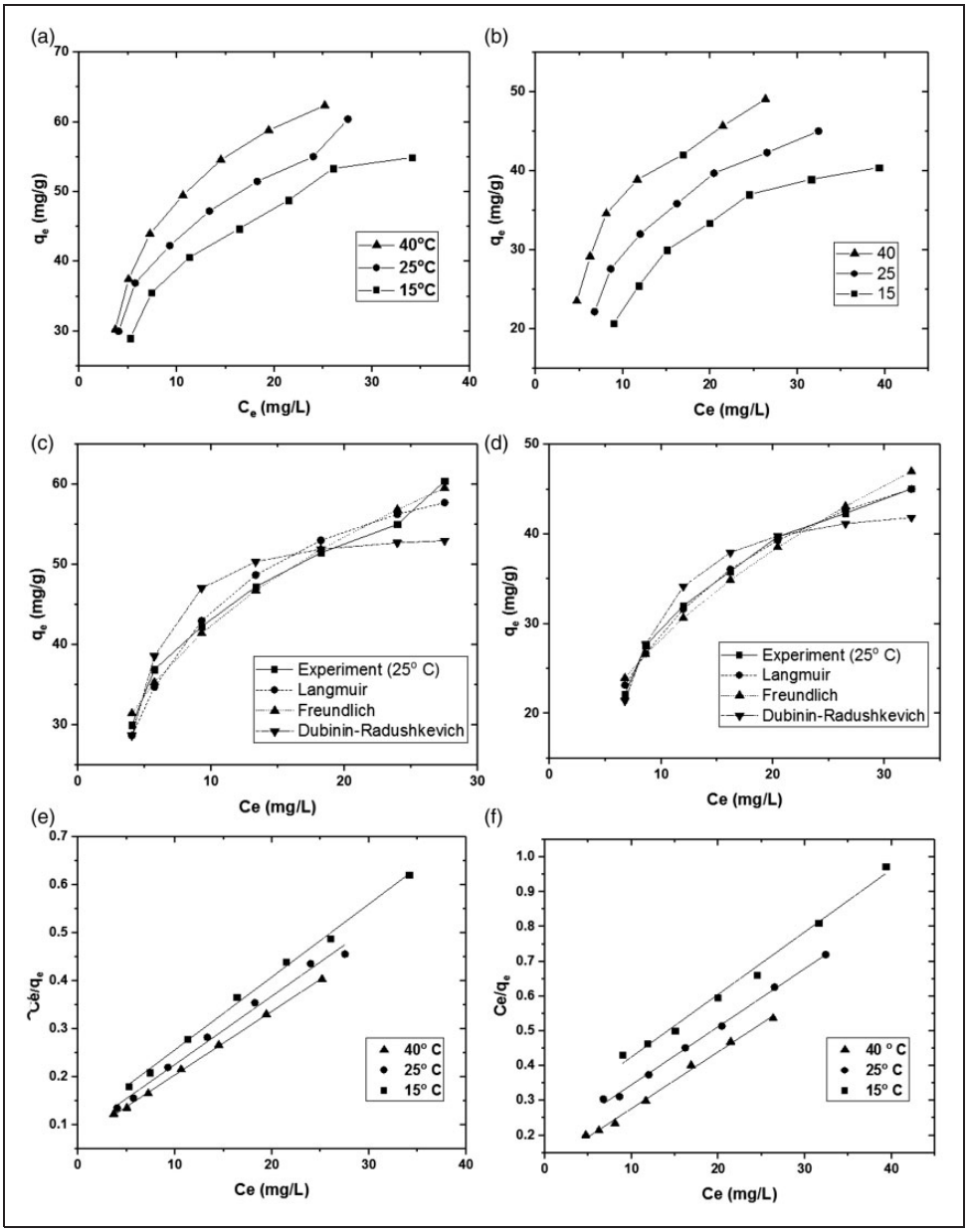


Figure 6. Effect of temperature for shale (a), coal (b); adsorption isotherms for shale (c), coal (d); Langmuir model at different temperatures for shale (e), coal (f).

Although R_L indicates that adsorption was a favoured mechanism in adsorption of vanadium on both sorbents, intra-particle diffusion model suggests that more than one mechanism is involved in the removal of vanadium on both adsorbents. Analysis of E suggests that chemisorption was also involved in sorption of vanadium on both

Table 3. Adsorption isotherm parameters of vanadium by coal waste and shale.

Coal Temp. (°C)	Q_m	Langmuir model			Freundlich model			Dubinin–Radushkevich model					
		B	R^2	R_L	K_F	$1n$	R^2	β	q_{RD}	R^2	E	ΔH^0	ΔS^0
15	55.56	.073	.992	.120	8.400	.447	.946	.0011	40.41	.975	21.31		
25	59.88	.094	.998	.097	10.57	.429	.966	.0060	43.31	.961	9.15	20.14	48.06
40	61.35	.143	.996	.066	14.00	.393	.951	.0029	46.46	.965	13.20		
Shale													
15	65.79	.146	.997	.064	17.52	.335	.980	.0035	51.16	.910	11.97		
25	69.93	.172	.991	.055	19.73	.333	.983	.0021	53.87	.892	15.39	7.31	9.56
40	75.19	.187	.999	.051	20.32	.362	.968	.0018	58.08	.943	16.62		

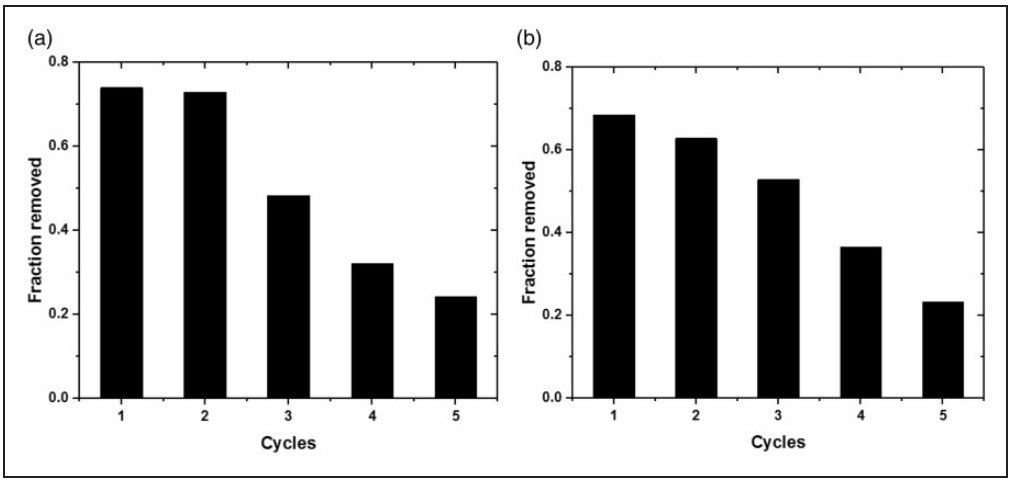


Figure 7. Adsorption–desorption cycles of shale (a) and coal (b).

adsorbents. The mean adsorption energy of coal waste ranges between 9 kJ/mol–21 kJ/mol and 11 kJ/mol–19 kJ/mol for shale. The positive value of ΔS^0 (48.06 J/mol/K for coal and 9.56 J/mol/K for shale) indicates an increasing randomness at the solid/liquid interface during vanadium adsorption.

Regeneration

According to Figure 7(a) and (b), after the second cycle, the adsorption rate reduced to 48.32% and 52.88% for shale and coal, respectively. This is attributed to a reduction in the specific surface area that directly affects the pore volume (Castrillo et al., 2015). In addition, during regeneration, a considerable amount of the adsorbents is lost (Doğan and Aydın, 2014). Keeping other factors (pH, concentration, temperature, and contact time) constant, reduction in adsorbent dose increases the equilibrium concentration, thus a reduction in removal efficiency.

Table 4. Comparison with other vanadium adsorbents.

Adsorbent	Capacity (mg/g)	
Multi-walled carbon nanotubes	375.94	Yu et al. (2017)
Chitosan–silica composite	244.51	Budnyak et al. (2015)
Magnetized natural zeolite polypyrrole	65.00	Mthombeni et al. (2016)
Bisphosphonate nano-cellulose	100.86	Sirviö et al. (2016)
Fe activated carbon	119.01	Sharififard and Soleimani (2015)
Zr(IV)-loaded orange juice residue	51.09	Hu et al. (2014)
Anion exchange (Amberjet^{TM} 4200 Cl)	48.9	Keränen et al. (2015)
Commercial-activated carbon	37.87	Sharififard and Soleimani (2015)
Starch waste sludge	37.17	Doğan and Aydın (2014)
Shale	75.19	This study
Coal waste	59.88	This study

Conclusion

In this study, the adsorption of vanadium on shale and unburnt coal waste was investigated. Both sorbents showed at least 60% adsorption of vanadium under optimal conditions (pH: 3; adsorbent quantity: 1.5 g/50 mL (coal waste), 1.2 g/50 mL (shale); vanadium concentration: 100 mg/L; temperature: 25 °C; contact duration: 24 hours). At a constant pH, adsorbent dose, temperature, and vanadium concentration, the adsorption of vanadium was rapid at the initial stage but slows gradually as equilibrium was attained. Shale has a better adsorption capacity than coal waste. This is attributed to good dispersibility of shale structure, large surface area, and bigger micropore volume compared to coal as seen from BET results. Although some adsorbents offer higher adsorption capacities (Table 4), usage of unburnt coal waste and shale which are readily available and cheap can be an economical breakthrough for treatment of wastewater and recovery of vanadium.

The adsorbents' performances are best achieved under elevated concentration of the acid. Therefore, there is a need for the modification of adsorbents to fit general wastewater pH and adsorption capacity improvements. However, environmental effects caused by chemical activation are remarkable in adsorption studies carried out with inexpensive and natural adsorbents. The yield values for vanadium removal and recovery of natural materials originating from coal enrichment processes are unique.

Acknowledgements

The authors acknowledge Michael Kayemba of Uzuri Health and Beauty, Gökhan Balcıoğlu of Environmental Engineering Laboratory, Istanbul University, and Joseph Wasswa of Weekat for the services rendered.

Declaration of Conflicting Interests

The author(s) declared no potential conflicts of interest with respect to the research, authorship, and/or publication of this article.

Funding

The author(s) received no financial support for the research, authorship, and/or publication of this article.

References

Balachandran M (2014) Role of infrared spectroscopy in coal analysis – An investigation. *American Journal of Analytical Chemistry* 5: 367–372.

Blissett RS and Rowson NA (2012) A review of the multi-component utilisation of coal fly ash. *Fuel* 97: 1–23.

Bolan N, et al. (2014) Remediation of heavy metal(loid)s contaminated soils – To mobilize or to immobilize? *Journal of Hazardous Materials* 266: 141–166.

Budnyak TM, et al. (2015) Adsorption of V (V), Mo (VI) and Cr (VI) oxoanions by chitosan–silica composite synthesized by Mannich reaction. *Adsorption Science & Technology* 33(6–8): 645–657.

Cappuyns V and Swennen R (2014) Release of vanadium from oxidized sediments: Insights from different extraction and leaching procedures. *Environmental Science and Pollution Research* 21(3): 2272–2282.

Cardoso AM, Horn MB, Ferret LS, et al. (2015) Integrated synthesis of zeolites 4A and Na-P1 using coal fly ash for application in the formulation of detergents and swine wastewater treatment. *Journal of Hazardous Materials* 287: 69–77.

Castrillo N, Mercado A and Bolzone C (2015) Reversibility studies of clay hydration degree in its natural and composite condition. *Procedia Material Science* 9: 135–141.

Chamley H (1989) *Clay Sedimentology*. Berlin: Springer.

Chen TC, Sapitan JF (Jaja) F, Ballesteros FC Jr, et al. (2015) Using activated clay for adsorption of sulfone compounds in diesel. *Journal of Cleaner Production* 124: 378–382.

Chen X-Y, Lan X-Z, Zhang Q-L, et al. (2010) Leaching vanadium by high concentration sulfuric acid from stone coal. *Transactions of Nonferrous Metals Society of China* 20: 123–126.

Clarke FW and Washington HS (1924) The composition of the Earth's crust. U.S Geological Survey 127.

Costigan M, Cary R and Dobson S (2001) Concise international chemical assessment document 29: Vanadium pentoxide and other inorganic vanadium compounds. Geneva: World Health Organization; ISBN 92 4 153029 4.

Doğan V and Aydın S (2014) Vanadium(V) removal by adsorption onto activated carbon derived from starch industry waste sludge. *Separation Science and Technology* 49(9): 1407–1415.

Fernández-Álvarez P, Vila J, Garrido JM, et al. (2007) Evaluation of biodiesel as bioremediation agent for the treatment of the shore affected by the heavy oil spill of the Prestige. *Journal of Hazardous Materials* 147(3): 914–922.

Fishman MJ and Skougstad MW (1964) Catalytic determination of vanadium in water. *Analytical Chemistry* 36: 1643–1646.

Gomes HI, Jones A, Rogerson M, et al. (2016) Vanadium removal and recovery from bauxite residue leachates by ion exchange. *Environmental Science and Pollution Research* 23(22): 23034–23042.

Goswami S, Pant HJ, Ambade RN, et al. (2017) Study of adsorption characteristics of Au(III) onto coal particles and their application as radiotracer in a coal gasifier. *Applied Radiation and Isotopes* 122: 127–135.

Haibin L and Zhenling L (2010) Recycling utilization patterns of coal mining waste in China. *Resources, Conservation and Recycling* 54(12): 1331–1340.

Herbert HJ, et al. (2016) Alteration of expandable clays by reaction with iron while being percolated by high brine solutions. *Applied Clay Science* 121–122: 174–187.

Höök M, Zittel W, Schindler J, et al. (2010) Global coal production outlooks based on a logistic model. *Fuel* 89(11): 3546–3558.

Hu Q, et al. (2014) Adsorptive recovery of vanadium(V) from chromium(VI)-containing effluent by Zr(IV)-loaded orange juice residue. *Chemical Engineering Journal* 248: 79–88.

infomine.com (2016) *Commodity and Metal Prices, Metal Price Charts – InvestmentMine*, vol. 3, pp. 6–13 September 2017).

Kacimi L, Cyr M and Clastres P (2010) Synthesis of α L-C2S cement from fly-ash using the hydrothermal method at low temperature and atmospheric pressure. *Journal of Hazardous Materials* 181(1–3): 593–601.

Keränen A, et al. (2015) Removal of nickel and vanadium from ammoniacal industrial wastewater by ion exchange and adsorption on activated carbon. *Desalination and Water Treatment* 53(10): 2645–2654.

Korbecki J, Baranowska-Bosiacka I, Gutowska I, et al. (2012) Biochemical and medical importance of vanadium compounds. *Acta Biochimica Polonica* 59(2): 195–200.

Leroy P and Revil A (2004) A triple-layer model of the surface electrochemical properties of clay minerals. *Journal of Colloid and Interface Science* 270(2): 371–380.

Llobet JM, Colomina MT, Sirvent JJ, et al. (1993) Reproductive toxicity evaluation of vanadium in male mice. *Toxicology* 80(2–3): 199–206.

Mohammadinia A, Arulrajah A, Horpibulsuk S, et al. (2017) Effect of fly ash on properties of crushed brick and reclaimed asphalt in pavement base/subbase applications. *Journal of Hazardous Materials* 321: 547–556.

Mohan S and Gandhimathi R (2009) Removal of heavy metal ions from municipal solid waste leachate using coal fly ash as an adsorbent. *Journal of Hazardous Materials* 169(1–3): 351–359.

Moskalyk RR and Alfantazi AM (2003) Processing of indium: A review. *Minerals Engineering* 16(8): 687–694.

Mthombeni NH, Mbakop S, Ochieng A, et al. (2016) Vanadium (V) adsorption isotherms and kinetics using polypyrrole coated magnetized natural zeolite. *Journal of the Taiwan Institute of Chemical Engineers* 66: 172–180.

Parasuraman A, Lim TM, Menictas C, et al. (2013) Review of material research and development for vanadium redox flow battery applications. *Electrochimica Acta* 101: 27–40.

Ren L, Zhang Y, Ying B, et al. (2015) Investigation of quartz flotation from decarburized vanadium-bearing coal. *Physicochemical Problems of Mineral Processing* 51(2): 755−767.

Ribeiro J, Flores D, Ward CR, et al. (2010) Identification of nanominerals and nanoparticles in burning coal waste piles from Portugal. *Science of the Total Environment* 408(23): 6032–6041.

Roberts GK, et al. (2016) 14-day toxicity studies of tetravalent and pentavalent vanadium compounds in Harlan Sprague Dawley rats and B6C3F1/N mice via drinking water exposure. *Toxicology Reports* 3: 531–538.

Sharififard H and Soleimani M (2015) Performance comparison of activated carbon and ferric oxide-hydroxide–activated carbon nanocomposite as vanadium(V) ion adsorbents. *The Royal Society of Chemistry* 5: 80650–80660.

Sirviö JA, Hasa T, Leiviskä T, et al. (2016) Bisphosphonate nanocellulose in the removal of vanadium(V) from water. *Cellulose* 23(1): 689–697.

Smith SC and Rodrigues DF (2015) Carbon-based nanomaterials for removal of chemical and biological contaminants from water: A review of mechanisms and applications. *Carbon* 91: 122–143.

Tarascon JM and Armand M (2001) Issues and challenges facing rechargeable lithium batteries. *Nature* 414(6861): 359–67.

Uddin MK (2017) A review on the adsorption of heavy metals by clay minerals, with special focus on the past decade. *Chemical Engineering Journal* 308: 438–462.

Ukwattage NL, Ranjith PG and Bouazza M (2013) The use of coal combustion fly ash as a soil amendment in agricultural lands (with comments on its potential to improve food security and sequester carbon). *Fuel* 109: 400–408.

United Nations (2016) *2014 Energy Statistics Yearbook* NY: United Nations Statistics Division.

Wang H, Wang X, Ma J, et al. (2017) Removal of cadmium (II) from aqueous solution: A comparative study of raw attapulgite clay and a reusable waste–struvite/attapulgite obtained from nutrient-rich wastewater. *Journal of Hazardous Materials* 329: 66–76.

Wang JP, He KR, Ding XM, et al. (2017) Effect of feeding and withdrawal of vanadium and vitamin C on egg quality and vanadium residual over time in laying hens. *Biological Trace Element Research* 177: 367–375.

Wei L, et al. (2017) Adsorption of Cu2 + and Zn2 + by extracellular polymeric substances (EPS) in different sludges: Effect of EPS fractional polarity on binding mechanism. *Journal of Hazardous Materials* 321: 473–483.

Yeom BY, Lee CS and Hwang TS (2009) A new hybrid ion exchanger: Effect of system parameters on the adsorption of vanadium (V). *Journal of Hazardous Materials* 166(1): 415–420.

Yu Y, Wei Q, Li J, et al. (2017) Removal of vanadium from wastewater by multi-walled carbon nanotubes. *Fullerenes, Nanotubes and Carbon Nanostructures* 25(3): 170–178.

Zakrzewska-Koltuniewicz G, Herdzik-Koniecko I, Cojocaru C, et al. (2014) Experimental design and optimization of leaching process for recovery of valuable chemical elements (U, La, V, Mo, Yb and Th) from low-grade uranium ore. *Journal of Hazardous Materials* 275: 136–145.

Zhang J, Dong W, Li J, et al. (2007) Utilization of coal fly ash in the glass-ceramic production. *Journal of Hazardous Materials* 149(2): 523–526.

Zhao Y, Zhang Y, Liu T, et al. (2013) Pre-concentration of vanadium from stone coal by gravity separation. *International Journal of Mineral Processing* 121: 1–5.